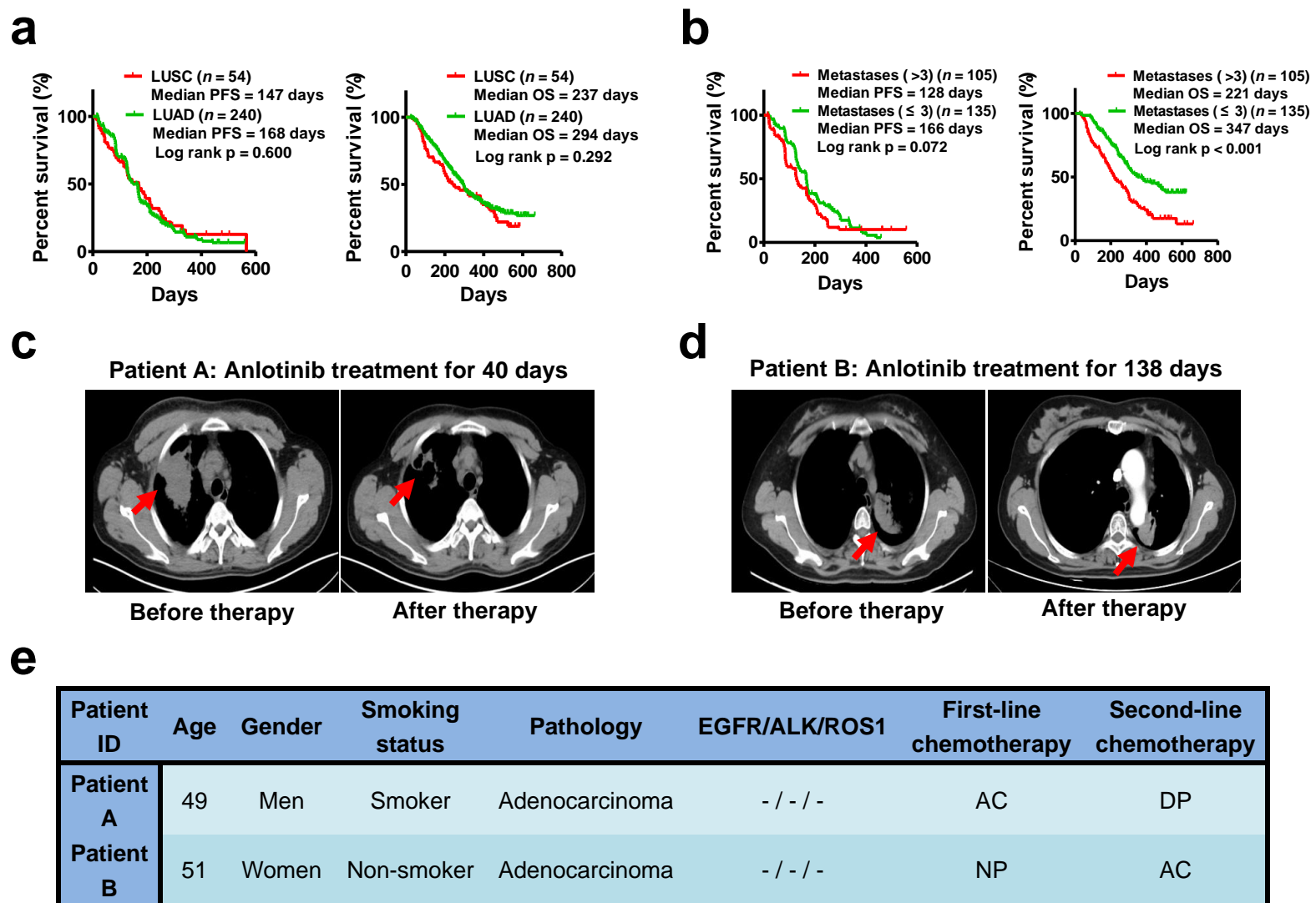


Supplementary Table 1

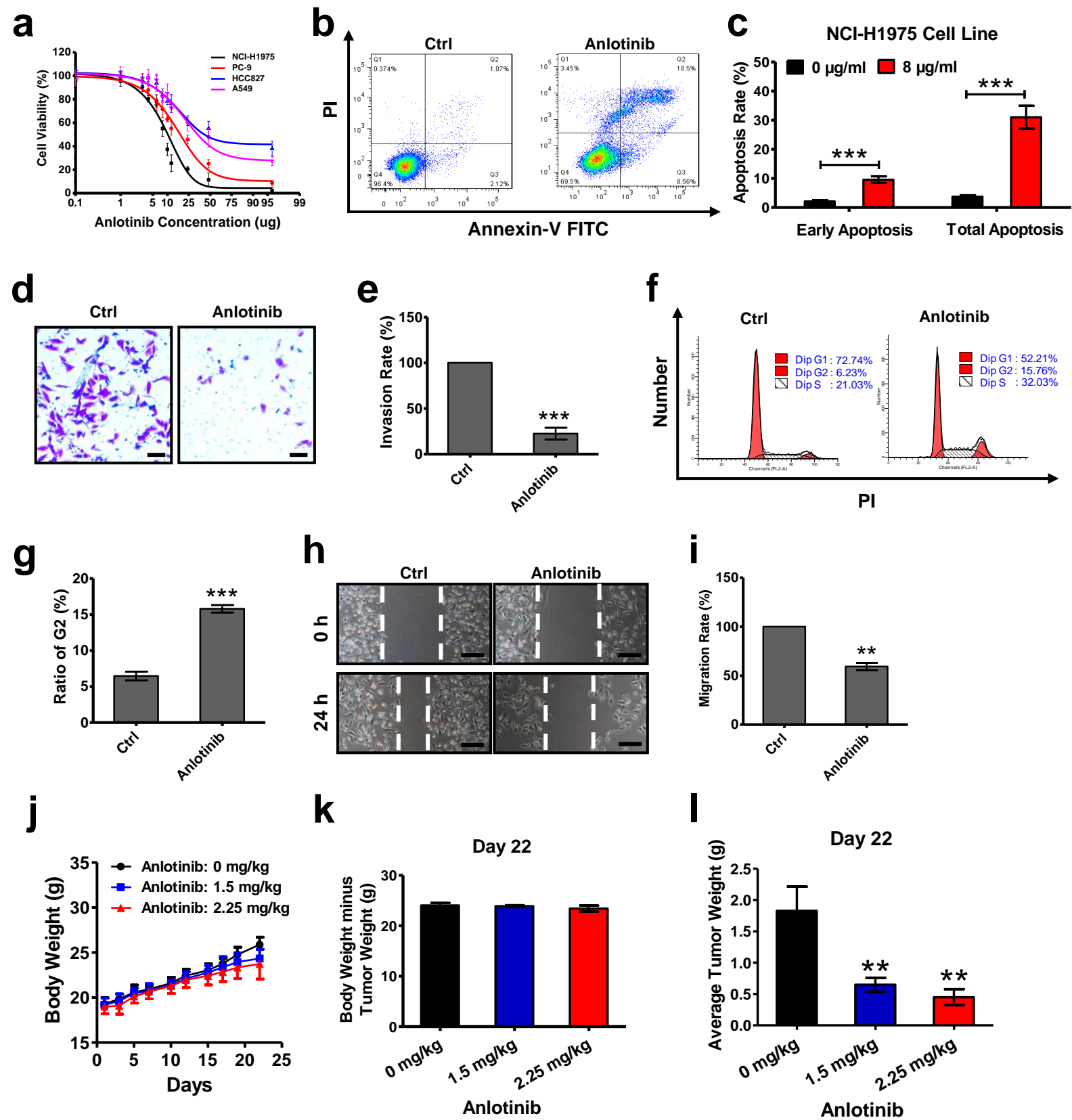
Status of NSCLC patients consisted of Anlotinib responder and Anlotinib nonresponder at their first biopsy.

Patients	Age	Gender	Smoking history	Type	Driver gene mutation	Number of Metastases
Responder 1	58	Female	Never	LUAD	EGFR ^{Exon 19-del, T790M} (+)	≤ 3
Responder 2	42	Male	Never	LUAD	ROS(+)	≤ 3
Responder 3	57	Female	Never	LUAD	EGFR ^{L858R} (+)	≤ 3
Responder 4	49	Female	Never	LUAD	Negative	≤ 3
Responder 5	52	Male	Never	LUAD	Negative	≤ 3
Responder 6	69	Male	Current/former	LUAD	Negative	≤ 3
Responder 7	62	Male	Never	LUAD	EGFR ^{L858R} (+)	> 3
Responder 8	52	Female	Never	LUAD	Negative	> 3
Responder 9	58	Male	Current/former	LUAD	EGFR ^{Exon 19-del} (+)	≤ 3
Responder 10	42	Male	Never	LUAD	Negative	≤ 3
Responder 11	66	Male	Current/former	LUSC	Negative	≤ 3
Responder 12	37	Male	Current/former	LUAD	Negative	> 3
Responder 13	52	Female	Never	LUSC	Negative	≤ 3
Responder 14	58	Female	Never	LUSC	Negative	> 3
Non-Responder 1	62	Male	Never	LUAD	Negative	> 3
Non-Responder 2	57	Male	Current/former	LUSC	Negative	> 3
Non-Responder 3	44	Female	Never	LUAD	Negative	≤ 3
Non-Responder 4	68	Male	Never	LUSC	Negative	≤ 3
Non-Responder 5	68	Male	Never	LUSC	Negative	≤ 3
Non-Responder 6	58	Male	Current/former	LUAD	Negative	> 3
Non-Responder 7	51	Male	Never	LUSC	EGFR ^{L858R} (+)	≤ 3
Non-Responder 8	50	Male	Current/former	LUAD	Negative	≤ 3
Non-Responder 9	52	Female	Never	LUAD	EGFR ^{Exon 19-del} (+)	> 3
Non-Responder 10	59	Female	Never	LUAD	Negative	> 3
Non-Responder 11	48	Female	Never	LUAD	Negative	≤ 3
Non-Responder 12	53	Female	Never	LUAD	Negative	> 3
Non-Responder 13	58	Female	Never	LUAD	Negative	> 3
Non-Responder 14	39	Male	Never	LUSC	Negative	≤ 3

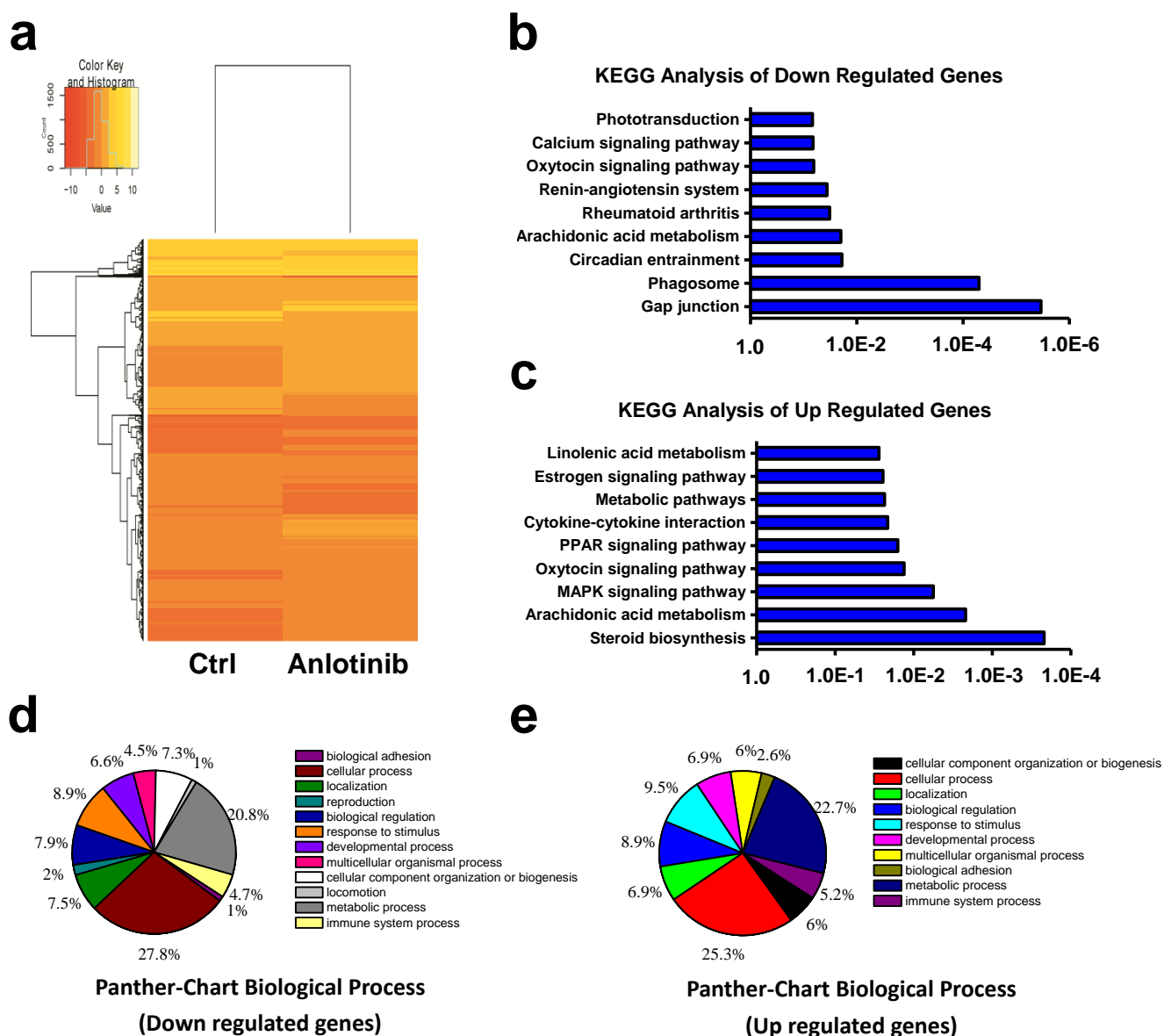


Supplementary Figure 1. Anlotinib response stratification analysis performed based on pathological types and number of metastases. (a) Kaplan-Meier plots of PFS and OS in NSCLC patients receiving anlotinib therapy by LUSC ($n = 54$) and LUAD ($n = 240$). Median PFS: 147 days (95% CI 111-183) vs 168 days (95% CI 155-181), median OS: 237 days (95% CI 191-283) vs 294 days (95% CI 274-314). (b) Kaplan-Meier plots of PFS in LUAD patients receiving anlotinib therapy by metastases > 3 ($n = 105$) and metastases ≤ 3 ($n = 135$). Median PFS: 128 days (95% CI 107-149) vs 166 days (95% CI 149-183), median OS: 221 days (95% CI 192-250) vs 347 days (95% CI 321-373). **Anlotinib therapy shrinks the tumour volume in**

refractory advanced LUAD patients without the driver gene mutation. (c, d) Two patients received anlotinib for 40 days and 138 days, respectively. The tumour of Patient A shrank significantly after 40 days of therapy, and the tumour of Patient B showed a partial response after 138 days of therapy. All images represent the maximum diameter of tumours. (e) Clinical characteristics of the two patients with advanced LUAD. AC regimen: pemetrexed plus carboplatin; DP regimen: docetaxel plus cisplatin; NP regimen: vinorelbine plus cisplatin; AC regimen: pemetrexed plus cisplatin.

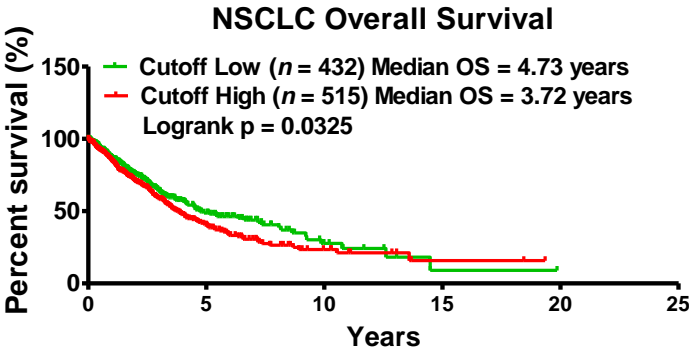


Supplementary Figure 2. Anlotinib-induced NCI-H1975 cell cytotoxic effects *in vitro* and *in vivo*. (a) Cell viabilities were evaluated by CCK8 after LUAD cell line exposure to Anlotinib for 24 hours. Bars = mean \pm SD, $n = 3$. (b, c) NCI-H1975 cells were exposed to anlotinib (8 μ g/ml) for 24 hours, and then, flow cytometry was used to detect apoptotic. Analyses of early apoptosis and total apoptosis were performed based on flow cytometric detection. Bars = mean \pm SD, $n = 3$, *** $P < 0.001$. (d, e) Transwell assays to assess NCI-H1975 cell invasion with or without anlotinib (2 μ g/ml) treatment. The invasion rate was calculated based on the transwell assays. Bars = mean \pm SD, $n = 3$, *** $P < 0.001$. (f, g) NCI-H1975 cells were exposed to anlotinib (6 μ g/ml) for 24 hours, and then, flow cytometry was used to detect the cell cycle distribution. The ratio of G2 was calculated based on flow cytometric detection. Bars = mean \pm SD, $n = 3$, *** $P < 0.001$. (h, i) NCI-H1975 cells were exposed to anlotinib (6 μ g/ml) for 24 hours, and the wound-healing scratch assay was performed to evaluate proliferation and migration. Bars = mean \pm SD, $n = 3$, ** $P < 0.01$. (j) Body weight was measured throughout the animal experiment. Bars = mean \pm SD, $n = 9$. (k) Body weight minus tumour weight was analysed at the end of the experiment. Bars = mean \pm SD, $n = 9$. (l) Measurement of tumour weight at the end of the experiment. Bars = mean \pm SD, $n = 9$, ** $P < 0.01$.

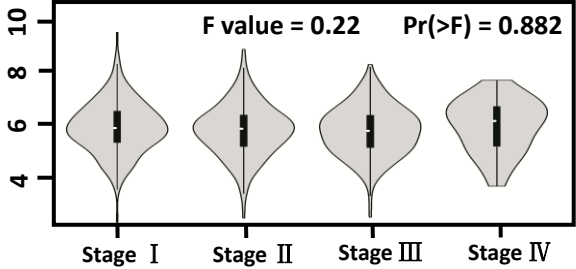


Supplementary Figure 3. Multiple signalling pathways and biological processes are disturbed after treatment with anlotinib (8 μ g/ml) in NCI-H1975 cells. (a) Heat map representation of differentially expressed genes in control-treated and anlotinib-treated NCI-H1975 cells. Red represents gene up-regulation, and blue represents gene down-regulation. (b, c) KEGG analysis of differentially expressed genes in the Ctrl vs. anlotinib. There were 1128 down-regulated genes (fold change > 2) and 636 up-regulated genes (fold change > 2) subjected to KEGG analysis. (d, e) Panther analysis of differentially expressed genes in the Ctrl vs. anlotinib. There were 1128 down-regulated genes (fold change > 2) and 636 up-regulated genes (fold change > 2) subjected to Panther analysis.

a



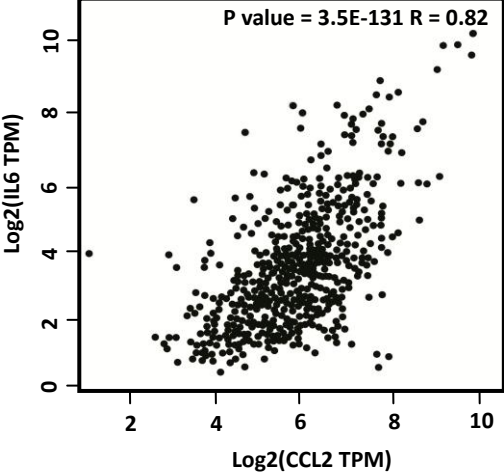
b



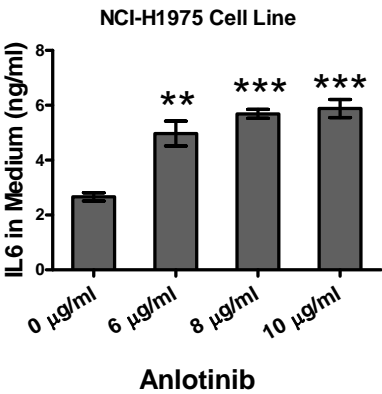
c

Gene Symbol	Gene ID	PCC
IL6	ENSG00000136244.11	0.82
CTD-2369P2.8	ENSG00000267607.1	0.75
RP11-79H23.3	ENSG00000261618.1	0.74
MMP19	ENSG00000123342.15	0.73
ARID5A	ENSG00000196843.15	0.73
SELE	ENSG00000007908.15	0.72
KDM6B	ENSG00000132510.10	0.68
ADAMTS4	ENSG00000158859.9	0.68
RP11-439L18.1	ENSG00000232618.1	0.68
RP11-64B16.2	ENSG00000213144.2	0.68

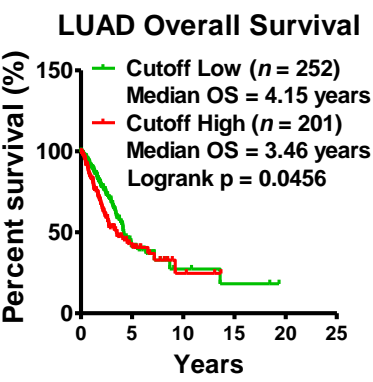
d



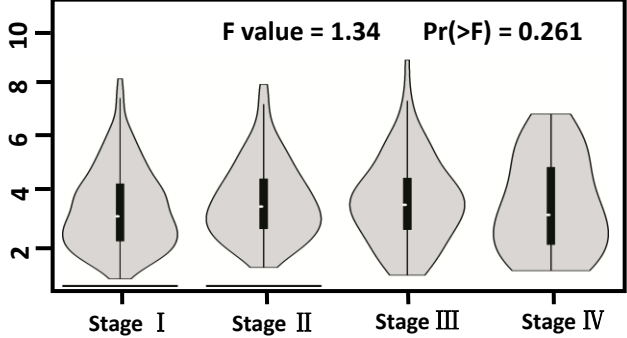
e



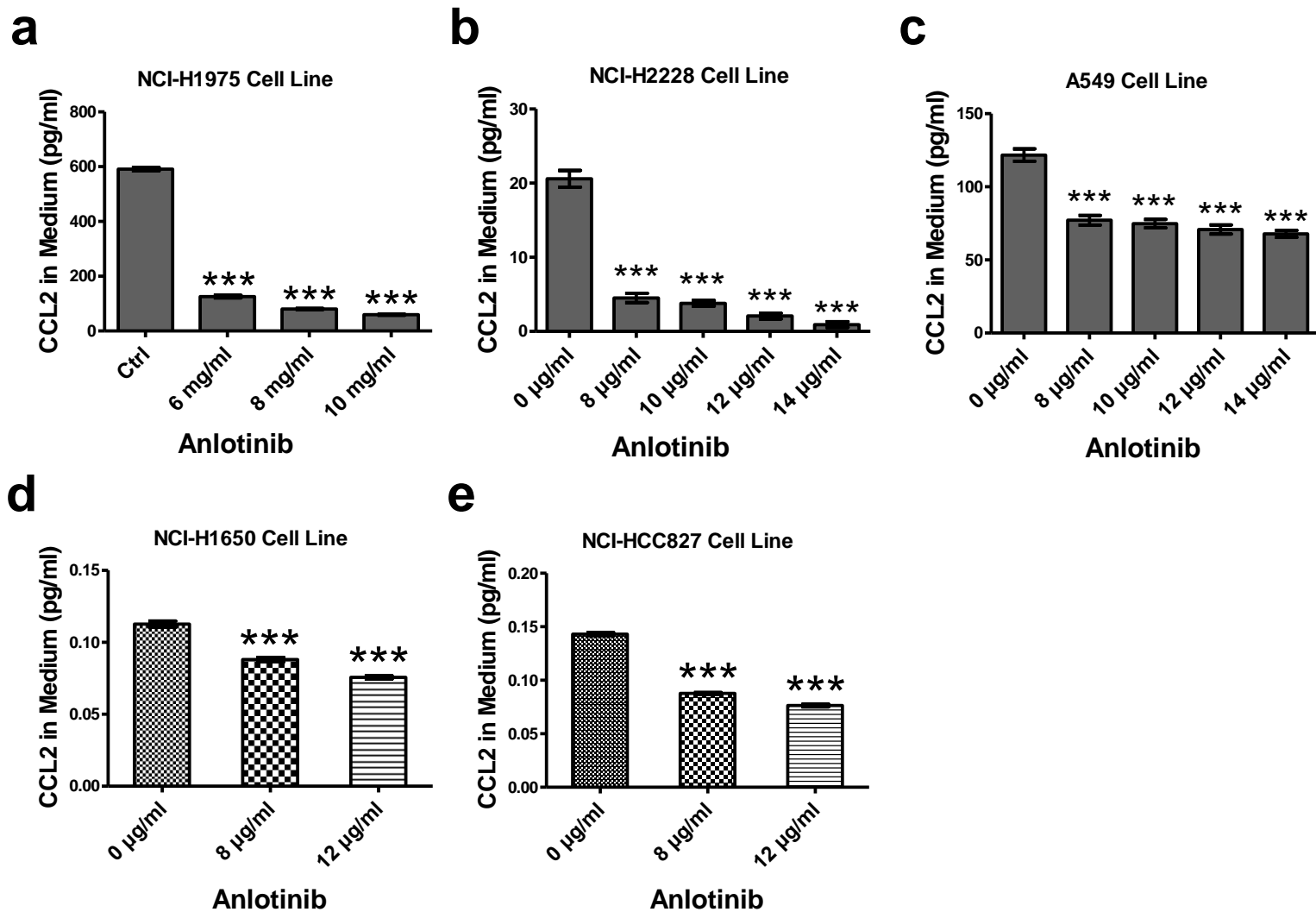
f



g

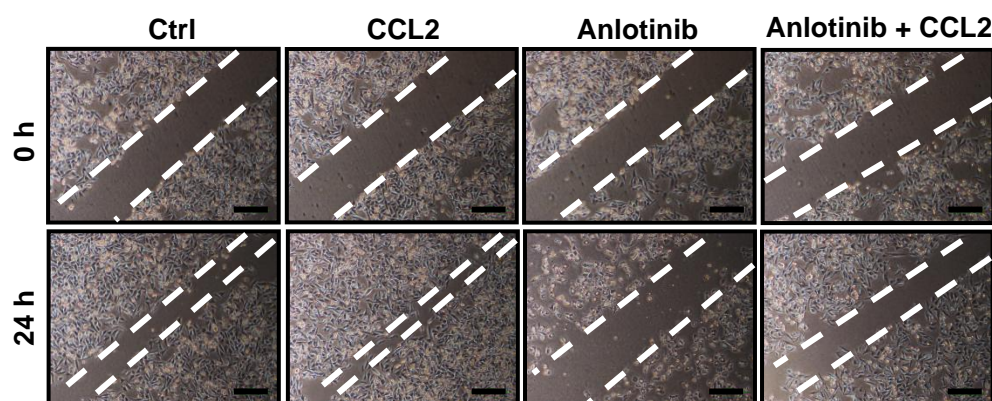
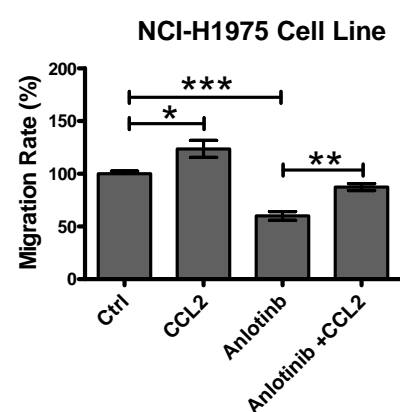
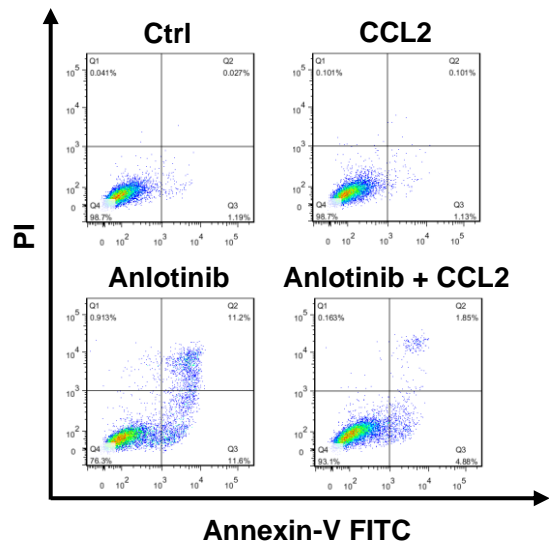
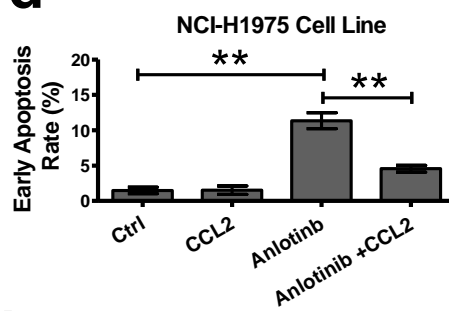
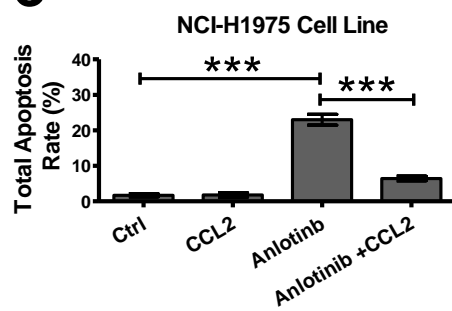
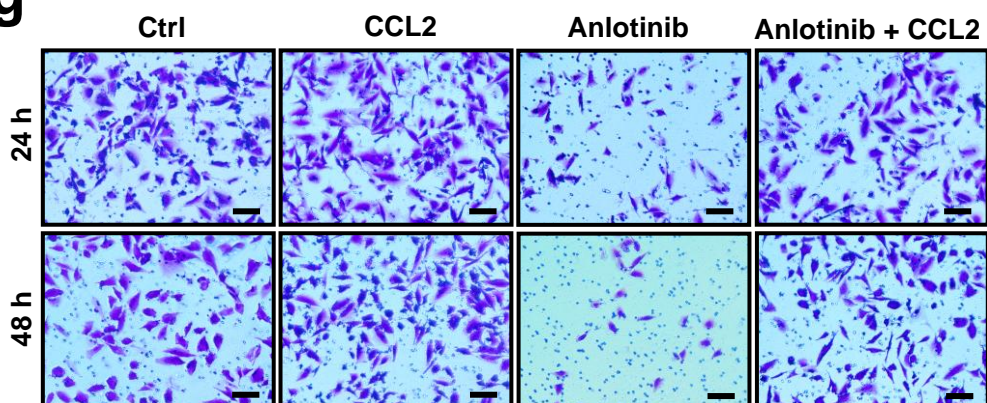
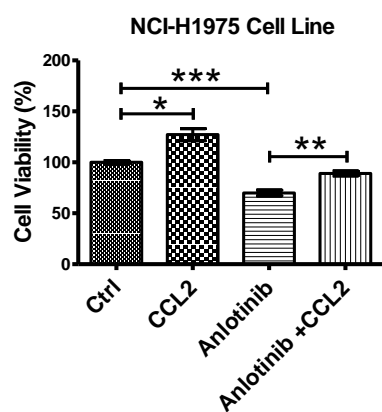
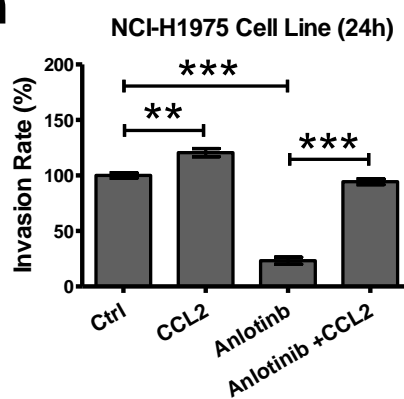
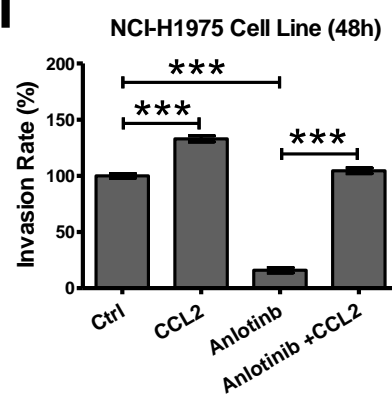


Supplementary Figure 4. Anlotinib-induced IL6 alterations are not associated with anlotinib-induced anti-angiogenesis. RNA-seq data from NSCLC patient biopsy samples ($n = 947$) and clinical data from NSCLC patients ($n = 947$) were analysed for the correlation of CCL2 expression and prognosis. (a) Kaplan-Meier plots of overall survival in NSCLC patients based on CCL2 expression stratification. Cut-off-high = 515; cut-off-low = 432. (b) CCL2 expression levels in NSCLC patients at different stages. (c) The top 10 co-expressed genes associated with CCL2 in LUAD patients. The significance of the correlation was determined using Pearson's correlation coefficient (PCC). (d) Correlation analysis of CCL2 and IL6 expression in LUAD patients. The significance of the CCL2-IL6 correlation was determined using PCC. (e) Alterations of IL6 levels after anlotinib (0 $\mu\text{g/ml}$, 6 $\mu\text{g/ml}$, 8 $\mu\text{g/ml}$ and 10 $\mu\text{g/ml}$) administration in NCI-H1975 cells. Bars = mean \pm SD, $n = 3$, $**P < 0.01$, $***P < 0.001$. (f) RNA-seq data from LUAD patient biopsy samples ($n = 453$) and clinical data from LUAD patients ($n = 453$) were analysed for the correlation of IL6 expression and prognosis. Cut-off-high = 201; cut-off-low = 252. (g) IL6 levels in LUAD patients at different stages.

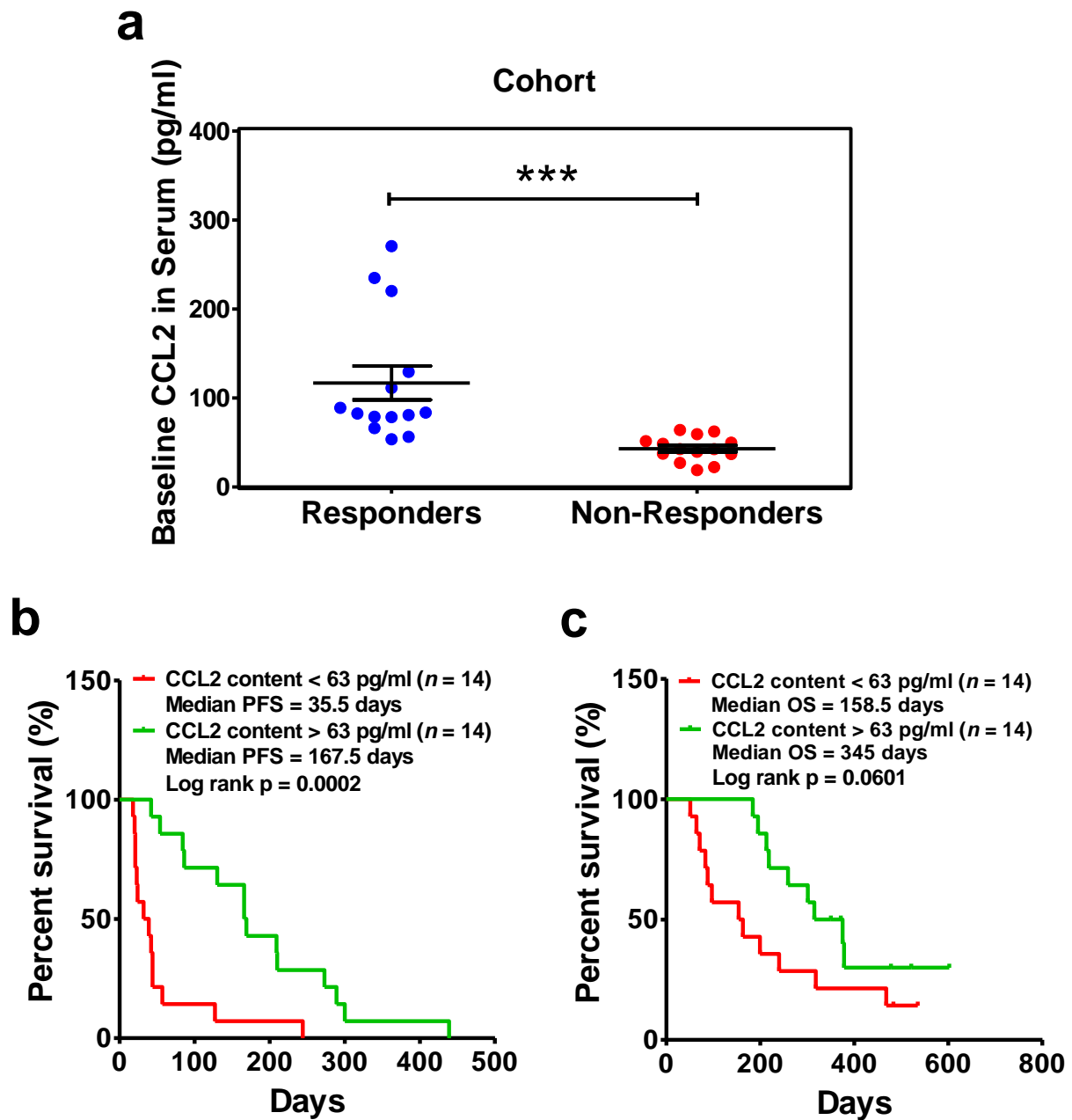


Supplementary Figure 5. Anlotinib inhibits CCL2 expression in LUAD cell lines.

LUAD cell lines (including NCI-H1975 cells, NCI-H2228 cells, A549 cells, NCI-H1650 cells and NCI-HCC827 cells) were exposed to anlotinib for 24 hours, and the contents of CCL2 in medium were measured by ELISA. (a) Alteration of the medium CCL2 concentration before and after anlotinib (6 µg/ml, 8 µg/ml and 10 µg/ml) administration in NCI-H1975 cells. Bars = mean \pm SD, $n = 3$, *** $P < 0.001$. (b, c) Alteration of the medium CCL2 concentration after anlotinib (0 µg/ml, 8 µg/ml, 10 µg/ml, 12 µg/ml and 14 µg/ml) administration in NCI-H2228 and A549 cells. Bars = mean \pm SD, $n = 3$, *** $P < 0.001$. (d, e) Alteration of the medium CCL2 concentration after anlotinib (0 µg/ml, 8 µg/ml and 12 µg/ml) administration in NCI-H1650 and NCI-HCC827 cells. Bars = mean \pm SD, $n = 3$, *** $P < 0.001$.

a**b****c****d****e****g****f****h****i**

Supplementary Figure 6. Replenishment of exogenous CCL2 offsets anlotinib-induced cytotoxicity in NCI-H1975 cells. (a, b) NCI-H1975 cells were exposed to CCL2 (50 ng/ml) and anlotinib (4 µg/ml), alone or together, for 24 hours. The wound-healing scratch assay was performed to evaluate the migration rate. Bars = mean ± SD, $n = 3$, $*P < 0.05$, $**P < 0.01$, $***P < 0.001$. (c-e) NCI-H1975 cells were exposed to CCL2 (50 ng/ml) and anlotinib (4 µg/ml), alone or together, for 24 hours. The apoptotic process was detected by flow cytometry. The ratios of early apoptosis and total apoptosis were analysed based on flow cytometric detection. Bars = mean ± SD, $n = 3$, $**P < 0.01$, $***P < 0.001$. (f) NCI-H1975 cells were exposed to CCL2 (50 ng/ml) and anlotinib (4 µg/ml), alone or together, for 24 hours. Cell viabilities were measured using the CCK8 kit. Bars = mean ± SD, $n = 3$, $*P < 0.05$, $**P < 0.01$, $***P < 0.001$. (g-i) NCI-H1975 cells were exposed to CCL2 (50 ng/ml) and anlotinib (2 µg/ml), alone or together, for 24 and 48 hours, respectively. Statistical analysis of the invasion rate based on transwell assays. Bars = mean ± SD, $n = 5$, $**P < 0.01$, $***P < 0.001$.



Supplementary Figure 7. Serum CCL2 levels at baseline predict the response to anlotinib in refractory advanced NSCLC patients. (a) Serum CCL2 levels at baseline in advanced refractory NSCLC patients consisted of anlotinib responders and anlotinib non-responder. Bars = mean \pm SD, $n = 14$, *** $P < 0.001$. (b) Kaplan-Meier curves of PFS stratified by serum CCL2 levels in advanced refractory NSCLC patients receiving anlotinib therapy. $n = 28$, cut-off-high: 50%; cut-off-low: 50%,

median PFS: 35.5 days (95% CI 0-71) vs 167.5 days (95% CI 104-231), log rank $P = 0.0002$. (c) Kaplan-Meier curves of OS stratified by the serum CCL2 levels in advanced refractory NSCLC patients receiving anlotinib therapy. $n = 28$, cut-off-high: 50%; cut-off-low: 50%, median OS: 158.5 days (95% CI 61-256) vs 345 days (95% CI 272-418), log rank $P = 0.0601$.

Supplementary Methods

Patients and samples. Patients bearing refractory advanced NSCLC were registered at Shanghai Chest Hospital, Tianjin Medical University Cancer Hospital, Henan Province Tumor Hospital, Peking Union Medical College Hospital, Linyi City Tumor Hospital, Shandong Province Tumor Hospital, Jilin Province Tumor Hospital, First Affiliated Hospital of Guangzhou Medical University, Chinese Academy of Medical Sciences Cancer Hospital, Lanzhou Military General Hospital, Qilu Hospital, Hunan Province Tumor Hospital, First Affiliated Hospital of Xi'an Jiaotong University, Tangdu Hospital, Beijing Chest Hospital of Capital Medical University, Jiangxi Province Tumor Hospital, The First Affiliated Hospital of Zhejiang University and Chongqing Cancer Hospital. The patients were confirmed to have advanced NSCLC (IIIB/IV stage) and had been receiving chemotherapy or driver gene inhibitors for at least two lines of therapy.[1-3] The patients received anlotinib as third-line therapy or beyond. Each cycle of medication for these patients consisted of anlotinib (12 mg/day) for two consecutive weeks and then discontinuation for one week. All patients received multiple cycles of anlotinib therapy until disease progression or intolerable toxicity occurred. Computed tomography (CT) was performed no more than 2 weeks before anlotinib therapy. After treatment initiation, tumours were evaluated once per cycle during the first two cycles and then once every two cycles. The patients who completed the anlotinib trial were followed up every eight weeks. Blood sample collections as well as CT evaluations were also performed. All patients provided written informed consent. The trial was registered at ClinicalTrials.gov under No. NCT02388919.

Cell culture. Procedures for cell culture were performed according to our previous studies.[4, 5] Briefly, the human LUAD cell lines NCI-H1975 (*EGFR*^{L858R, T790M} mutation), PC-9 (*EGFR*^{L858R} mutation), HCC-827 (*EGFR*^{Exon 19 deletion} mutation), A549 (*EGFR*^{wild type}), NCI-H2228 (EML4-ALK fusion) and NCI-H1650 (*EGFR*^{Exon 19 deletion}, PTEN loss) were obtained from ATCC: The Global Bioresource Center (<https://www.atcc.org/>). All cell lines were validated to contain no mycoplasma

contamination using the TransDetect PCR Mycoplasma Detection Kit (TransGen, China). Cells were maintained in RPMI 1640 medium (Gibco, USA) supplemented with 10% foetal bovine serum (FBS) (Gibco, USA) and 100 units/ml of penicillin and streptomycin (Gibco, USA). The cells were incubated at 37 °C in a humidified atmosphere of 5% CO₂.

Cell viability analysis. Cells were cultured at 1500 cells per well in 96-well plates for 24 hours and then treated with anlotinib for 24 hours. The cell counting kit 8 (CCK8) (Dojindo, Japan) was used to evaluate cell viability according to the manufacturer's protocol. Cell viabilities were calculated by measuring the optical density at 450 nm using a spectrophotometric plate reader (Bio-Tek, USA). The absorbance of the control sample was set at 100% viability, and the absorbance of cell-free wells containing medium was set at zero. All cell viability results were tested in three independent experiments.

Flow cytometric analysis. To analyse apoptotic cells, the Annexin V-FITC/PI Apoptosis kit (Zoman Biotechnology Co., Ltd, China) was used to determine the phosphatidyl serine content and membrane integrity of each cell. The detailed procedures were performed according to our previous studies.[4, 5] Cells were stained with Annexin V-FITC and PI simultaneously and then detected by flow cytometry (BD LSRFortessa, USA). PI-positive cells were designated as end-stage apoptotic cells, and FITC-positive cells were designated as early-stage apoptotic cells. To evaluate anlotinib-induced apoptosis, 5×10^5 NCI-H1975 cells were cultured in 6-well plates for 24 hours and then treated with anlotinib (8 µg/ml) for 24 hours. To assess whether replenishment with exogenous human recombinant CCL2 (Pepro Tech, USA) could offset anlotinib-induced apoptosis, 5×10^5 NCI-H1975 cells were cultured in 6-well plates for 24 hours and then were exposed to CCL2 (50 ng/ml) and anlotinib (6 µg/ml), alone or together, for 24 hours. To analyse the cell cycle, PI (Aladdin, China) was used to stain anlotinib-treated and non-treated cells. All prepared samples were detected by flow cytometry (BD LSRFortessa, USA). The ratios of G1-phase, G2-phase and S-phase were analysed based on flow cytometric detection.

Cell invasion. Invasion assays were performed using a transwell filter (8- μ m pore size; Corning, USA). Transwell membranes were coated with Matrigel matrix (diluted with 1:8; Corning, USA). NCI-H1975 cells were starved overnight in RPMI 1640 (Gibco, USA), then were seeded onto the top precoated chamber (5×10^4 cells per well for 24 hours evaluation; 2×10^4 cells per well for 48 hours evaluation) in 100 μ l of FBS-free medium. RPMI 1640 medium with 15% FBS was placed in the bottom chamber. After a 24-or 48-hour incubation at 37 °C in 5% CO₂, the lower surface of the membrane with invasive NCI-H1975 cells was fixed with 3.7% paraformaldehyde for 30 minutes, stained with 0.1% crystal violet for 2 hours, and then washed twice with PBS. Fluorescence microscopy (Nikon, Japan) was used to capture images and quantify the number of cells per field.

Wound-healing scratch assay. Wound-healing scratch assays were performed to assess the NCI-H1975 cell migration. A total of 1×10^6 cells were cultured in 6-well plates for 24 hours and starved overnight in RPMI 1640 (Gibco, USA); then, a scratch wound was created using 200- μ l pipette tip. The medium was replaced with fresh RPMI 1640 medium (Gibco, USA) supplementary with 10% FBS. For evaluation anlotinib-induced migration inhibition, samples were treated with anlotinib (6 μ g/ml) for 24 hours. For assessment CCL2-induced migration recovery, samples were treated with anlotinib (4 μ g/ml) and human recombinant CCL2 (50 ng/ml), alone or together, for 24 hours. Images of cell migration were captured by microscopy (Nikon, Japan), and the migration rate was calculated based on the change of wound width.

Cell immunofluorescence assays. NCI-H1975 cells were cultured in a glass-bottom cell culture dish (NEST, USA) for 24 hours and then treated with anlotinib (4 μ g/ml) and CCL2 (50 ng/ml), alone or together, for 24 hours. The cell culture dishes were washed two times with PBS, fixed with 4% PFA for 30 minutes, and blocked with blocking buffer (5% goat serum and 0.3% Triton-100) for 1 hour. Primary antibodies against MMP9 (1:200, Abcam, USA), CD31 (1:200, BD/PMG, USA) and Ki67 (1:200, Abcam, USA) were incubated to bind specific proteins, followed by anti-rabbit Alexa Fluor®647-conjugated (1:1000, CST, USA) and anti-mouse Alexa

Fluor®488-conjugated (1:1000, CST, USA) secondary antibodies. Finally, all samples were stained with Hoechst33324 for nuclear observation. Fluorescently labelled cells were observed using confocal laser scanning microscopy (CLSM) (Nikon, Japan).

Animal experiments. Experiments using Balb/c nude mice (SLAC Laboratory Animal) were performed according to national guidelines for welfare. All of the mice used in the present study were female and aged 4-6 weeks. All mice had free access to food and water throughout the experimental period. To induce the NCI-H1975-derived xenograft model, 5×10^6 NCI-H1975 cells in Reduced Matrigel® Matrix Growth Factor (Corning, USA) were subcutaneously injected in the right fore-lateral abdomen.

To assess the anti-tumour effect of anlotinib, the mice were divided into three groups: Ctrl, anlotinib 1 and anlotinib 2. The anlotinib treatments (anlotinib 1, 1.5 mg/kg and anlotinib 2, 2.25 mg/kg) were administered 14 days after NCI-H1975 cell injection via gavage for two consecutive weeks and then discontinued for one week. Saline was administered in the Ctrl group. To evaluate whether the replenishment of exogenous CCL2 could recover anlotinib-induced anti-angiogenesis *in vivo*, the mice were divided into three groups: Ctrl, anlotinib and anlotinib + CCL2. Anlotinib (2.5 mg/kg) treatment was described above. CCL2 (R&D systems, USA; 5 µg/kg, iv, qod) treatment was performed via tail intravenous injection.

Body weight and tumour volume were measured three times per week. Tumour volume was calculated based on the following formula: $\text{volume} = \text{length} \times \text{width}^2/2$. The fold change in tumour growth was calculated based on the following formula: $\text{fold change} = \text{tumour volume of Day } n / \text{tumour volume of Day } 1$. Serum was collected on Day 5 and Day10. When the tumour volume of any mouse reached the maximal value allowed under our institutional protocol, serum collection and tumour tissue collection were performed immediately for all mice. Tumours were collected and weighed. All serum samples were stored at -80 °C. Half of the tumour samples from each mouse were fixed using 4% PFA, and the other half were stored at -80 °C.

Histology analysis. Tumour tissue was stored at -80 °C (Thermo, USA) and then sectioned at a thickness of 8-10 µm using a freezing microtome (Leica, Germany). For general observations, sections on glass slides were dehydrated and then stained with haematoxylin and eosin (H&E). For immunofluorescent histochemical observation, the sections on glass slides were incubated with primary antibody against CD31 (1:50, BD/PMG, USA), Ki67 (1:200, Abcam, USA) or MMP9 (1:100, Abcam, USA) and then with Alexa Fluor®647-conjugated secondary antibody. For vessel staining, lectin (1:100, VECTOR, USA) was incubated with the samples for 24 hours. Finally, the slides were stained with Hoechst33324 for nuclear observations. All fluorescently labelled slides were observed using confocal laser scanning microscopy (CLSM) (Nikon, Japan).

RNA-seq library. NCI-H1975 cells were cultured in 6-well plates for 24 hours and then treated with anlotinib (8 µg/ml) for 24 hours. TRIzol reagent (Life Technologies, Inc., USA) was used to lyse cell samples, followed by total RNA isolation using standard procedures. mRNA was isolated using the Oligotex mRNA Mini Kit (Qiagen, Germany). Residual genomic DNA was degraded by adding DNase (NEB, USA), followed by incubation for 30 minutes at 37 °C. Next, 100 ng mRNA from each sample was reverse-transcribed into cDNA and fragmented into 100-300-bp pieces. The NEBNext Ultra Directional RNA Library Prep Kit (NEB, USA) was used to end-repair and adapter-ligate the fragmented cDNA. The samples were amplified using 10 cycles in a thermal cycler in PCR Master Mix supplemented with Q5 High-Fidelity DNA Polymerase (NEB, USA). The PCR products were quantified using an Agilent 2100 bioanalyzer (Agilent, USA), and standard paired-end sequencing with 75-bp reads was performed using the Illumina Next500 (Illumina, USA) sequencing platform. The raw data for this study are available in the EMBL database under accession number E-MTAB-5997: <http://www.ebi.ac.uk/arrayexpress/>.

Analysis of RNA-seq raw data. The raw sequencing reads were extracted and analysed using Illumina software. The sequencing quality was detected using FastQC software. All qualified sequence tags were mapped to the reference genome (hg38) by

TopHat.[6] Cufflinks was used to characterize the differential transcription pattern. Biases in library preparation were taken into account. The gene expression level was measured by the reads per kilo-base of transcript per million mapped reads (FPKM). To analyse the gene expression difference between anlotinib-treated samples and the Ctrl sample, we selected genes with an expression level exhibiting at least a two-fold change. According to the analytical method, a $\log_2^{\text{Fold Change}} > 1$ represented a gene expression level that was least two-fold up-regulated, and a $\log_2^{\text{Fold Change}} < -1$ represented a gene expression level that was at least two-fold down-regulated.

Functional annotation, pathway analysis and Panther analysis. Analyses of gene function clusters and pathway clusters were performed using a public bioinformatics resource platform named Database for Annotation, Visualization and Integrated Discovery (DAVID, <https://david.ncifcrf.gov/>).[7] Briefly, a list of differentially expressed genes was uploaded to DAVID Bioinformatics Resources 6.7, and gene ontology (GO) cluster and Kyoto Encyclopaedia of Genes and Genomes (KEGG) pathway cluster analyses were performed. Panther analysis was also performed using the Panther Classification System (<http://www.pantherdb.org/>).

mRNA expression analysis. NCI-H1975 cells were cultured in 6-well plates for 24 hours and then treated with anlotinib (8 $\mu\text{g/ml}$) for 24 hours. Total RNA isolation was performed as previously mentioned. RNA was purified using the RNeasy kit (Qiagen, Germany) according to the manufacturer's protocol. Reverse transcription was performed using random primers and SuperScrip®III Reverse Transcriptase (Invitrogen, USA). RT-qPCR was performed to analyse target gene expression using SYBR Green PCR Mix (Thermo, USA). GAPDH was used as a reference control for normalization. The obtained values were expressed as n-fold changes in regulation compared with the control by applying the $2^{-\Delta\Delta\text{Ct}}$ method of relative quantification. The primer sequences used in the present study for RT-qPCR detection were as follows: *CCL2*: forward 5'-3' CAGCCAGATGCAATCAATGCC, reverse 5'-3' TGGAATCCTGAACCCACTTCT; *IL6*: forward 5'-3' AGACAGCCACTCACCTCTTC, reverse 5'-3' AGTGCCTCTTTGCTGCTTTC;

PECAM1(CD31): forward 5'-3' CCTTCAACAGAGCCAACCAC, reverse 5'-3' GGCCGCAATGATCAAGAGAG; *MKI67 (Ki67)*: forward 5'-3' CACGAGACGCCTGGTTACTA, reverse 5'-3' TGACACAACAGGAAGCTGGA; *MMP-1*: forward 5'-3' TCATGCTTTTCAACCAGGCC, reverse 5'-3' TCATGAGCTGCAACACGATG; *MMP-2*: forward 5'-3' TGCTCCACCACCTACAACCTT, reverse 5'-3' GCAGCTGTCATAGGATGTGC; *MMP-3*: forward 5'-3' CCTGGAAATGTTTTGGCCCA, reverse 5'-3' GGCTGAGTGAAAGAGACCCA; *MMP-9*: forward 5'-3' TGCCACTTCCCCTTCATCTT, reverse 5'-3' CGTCCTGGGTGTAGAGTCTC; *MMP-19*: forward 5'-3' ACTTCCAGTCTCAGGTCAGC, reverse 5'-3' GCAGGTTCAAGATGCGGAAA; and GAPDH: forward 5'-3' AGGTCGGAGTCAACGGATTT, reverse 5'-3' TGACAAGCTTCCCGTTCTCA.

ELISA. All ELISA kits for CCL2 and IL6 detection were purchased from eBioscience. For the *in vitro* experiments, the culture media of NCI-H1975, NCI-H2228, A549, NCI-H1650 and NCI-HCC827 cells were collected after anlotinib treatment. For the *in vivo* experiments, serum was obtained at different time points after anlotinib administration. The tumour tissue homogenate was collected at the end of the animal experiment. CCL2 levels were evaluated using mCCL2 Platinum ELISA (eBioscience, USA) for mice and hCCL2 Platinum ELISA (eBioscience, USA) for humans. IL-6 levels were assessed using hIL6 Platinum ELISA (eBioscience, USA). All experimental procedures were performed according to the manufacturer's protocol.

Analysis of the TCGA cohort. RNA-seq data and clinical data for NSCLC (including LUAD and LUSC) were downloaded from the TCGA data portal (<https://cancergenome.nih.gov/>). In total, 453 clinical data and RNA-seq data accounted for LUAD, and 494 clinical data and RNA-seq data accounted for LUSC. All data were parsed using a custom R function. The FPKM expression values were transformed to log2 counts per million using the voom function from the limma R

package. Cut-off values for CCL2 and IL6 were defined using the “Ward method”. Co-expression analysis of CCL2 and correlation analysis of CCL2-IL6 were performed according to the Gene Expression Profiling Interactive Analysis (GEPIA) (<http://gepia.cancer-pku.cn/index.html>).

References

1. Han BH, Li K, Wang QM, et al. Effect of Anlotinib as a Third-Line or Further Treatment on Overall Survival of Patients With Advanced Non–Small Cell Lung Cancer The ALTER 0303 Phase 3 Randomized Clinical Trial. *JAMA Oncol.* 2018; doi:10.1001/jamaoncol.2018.3039.
2. Han BH, Li K, Zhao YZ, et al. Anlotinib as a third-line therapy in patients with refractory advanced non-small-cell lung cancer: a multicentre, randomised phase II trial (ALTER0302). *Br J Cancer.* 2018; doi: 10.1038/bjc.2017.478.
3. Han BH, Li K, Wang QM, et al. Efficacy and safety of third-line treatment with anlotinib in patients with refractory advanced non-small-cell lung cancer (ALTER-0303): a randomised, double-blind, placebo-controlled phase 3 study. *Lancet Oncol.* 2017; 18: S3-S3.
4. Zhang XL, Wu J, Wang J, et al. Integrative epigenomic analysis reveals unique epigenetic signatures involved in unipotency of mouse female germline stem cells. *Genome Biol.* 2016; 17(1): 162.
5. Lu J, Chen J, Xu N, et al. Activation of AIFM2 enhances apoptosis of human lung cancer cells undergoing toxicological stress. *Toxicol Lett.* 2016; 258: 227-36.
6. Trapnell C, Roberts A, Goff L, et al. Differential gene and transcript expression analysis of RNA-seq experiments with TopHat and Cufflinks. *Nat Protoc.* 2012; 7(3): 562-78.
7. Huang DW, Sherman BT, Tan Q, et al. DAVID Bioinformatics Resources: expanded annotation database and novel algorithms to better extract biology from large gene lists. *Nucleic Acids Res.* 2007; 35: W169-75.